Title

Shear-activated chemisorption and association of cyclic organic molecules

Journal

Faraday Discussions, 241(0)

ISSN

1359-6640

Authors

Bhuiyan, Fakhrul H
Li, Yu-Sheng
Kim, Seong H
et al.

Publication Date

2023-01-05

DOI

10.1039/d2fd00086e

Peer reviewed

https://doi.org/10.1039/D2FD00086E

ARTICLE

Shear-Activated Chemisorption and Association of Cyclic Organic Molecules

Fakhrul H. Bhuiyan,[a] Yu-Sheng Li,[b] Seong H. Kim [b] and Ashlie Martini *[a]

Mechanochemical activation has created new opportunities for applications such as solvent-free chemical synthesis, polymer processing, and lubrication. However, mechanistic understanding of these processes is still limited because the mechanochemical response of a system is a complex function of many variables, including the direction of applied stress and the chemical features of the reactants in non-equilibrium conditions. Here, we studied shear-activated reactions of simple cyclic organic molecules to isolate the effect of chemical structure on reaction yield and pathway. Reactive molecular dynamics simulations were used to model methylcyclopentane, cyclohexane, and cyclohexene subject to pressure and shear stress between silica surfaces. Cyclohexene was found to be more susceptible to mechanochemical activation of oxidative chemisorption and subsequent oligomerization reactions than either methylcyclopentane or cyclohexane. The oligomerization trend was consistent with shear-driven polymerization yield measured in ball-on-flat sliding experiments. Analysis of the simulations showed the distribution of carbon atom sites at which oxidative chemisorption occurred and identified the double bond in cyclohexene as being the origin of its shear susceptibility. Lastly, the most common reaction pathways for association were identified, providing insight into how the chemical structures of the precursor molecules determined their response to mechanochemical activation.

Introduction

Mechanochemistry describes chemical reactions that are assisted or driven by mechanical force. Although not as well understood as thermal-, photo-, and electro-activation, mechanical activation is now considered to be a promising technique for many manufacturing and synthesis processes. By eliminating or minimizing the need for a solvent or an external heating source, mechanochemistry has opened exciting new alternatives to conventional synthesis technologies that are simpler, faster, and greener.[1–3] Mechanochemistry also plays a critical role in manufacturing and engineering processes, including chemical mechanical polishing,[4] polymer processing,[5,6] heat assisted magnetic recording,[7] and lubrication.[8,9] Depending on the application, the mechanical stress required to induce the relevant mechanochemical reactions can be provided through grinding, compression, tension, or shearing. Regardless of the method used to supply mechanical energy to chemical bonds, the mechanochemical response of a system is difficult to predict due to the complexity of many variables involved, particularly, the magnitude and direction of applied stress and the chemical features of the reactants under non-equilibrium conditions.

The ability of stress to activate a chemical reaction depends not only on the magnitude of the stress but also direction in which it is applied relative to the reaction coordinate. This phenomenon has been observed in many studies involving application-relevant chemical species. For example, zinc dialkyldithiophosphate (ZDDP), a common antiwear lubricant additive, is known to create a protective film on metallic surfaces through chemical reactions with the surface. In-situ atomic force microscopy (AFM) experiments of ZDDP films on metallic surfaces showed that the tribofilm growth rate increased exponentially with contact stress following a stress-assisted thermal activation model.[10] Later, ball-on-flat tribometer measurements on ZDDP tribofilm growth revealed that the film growth is driven mainly by shear stress rather than normal stress.[11,12] In fact, mechanochemical activation of molecules can require a very specific stress condition at a molecular level. For example, spiropyran, a common mechanochromic mechanophore, can be mechanically activated only if the applied force stretches the C-O bond, which is known to be the weak link of the mechanophore.[13] Other chemical systems have been shown to respond similarly to tensile stress that activates the reaction by elongating the mechanophore.[6] Such studies have demonstrated that the effectiveness of mechanical activation can vary dramatically based on the direction of stress.

The chemical features of the reactants also affect mechanochemical processes. For instance, it was shown that secondary sulfur-free zinc dialkylphosphates (ZDPs) have faster

[a] Department of Mechanical Engineering, University of California Merced, 5200 N. Lake Road, Merced, California 95343, United States
[b] Department of Chemical Engineering and Materials Research Institute, Pennsylvania State University, University Park, Pennsylvania 16802, United States
* amartini@ucmerced.edu

Electronic Supplementary Information (ESI) available: Simulation results for all precursors at 300 K at three pressures. Activation volume calculation. Simulation results at 900 K with no pressure or shear.

film growth rates than primary ZDPs.[14] Similar experiments on ZDDP revealed that film growth rates were dependent on the additive's alkyl substituents, where additives with secondary alkyl substituents formed films faster than additives with primary substituents.[12,14] The effect of substituents on polymer mechanochemistry has also been investigated. A study on the macroscopic fracture of poly(ethylene glycol) gels embedded with cis-diaryl or cis-dialkyl linked cyclobutane showed that the critical strain for fracture and tearing energy varied significantly between the two mechanophores.[15] Further, the mechanochromic properties of spiropyran could be tuned by inserting suitable substituents to the mechanophores.[16] These studies have shown that even subtle differences between reactants can affect how mechanical stress activates chemical reactions.

To understand the interrelated effects of stress and molecular features on mechanochemical reactions, many studies have focused on simple organic molecules and substituents as model systems. For example, mechanochemical cycloreversion of perfluorocyclobutane (PFCB) to trifluorovinyl ethers was investigated in ultrasound experiments.[17] Mechanical stress was shown to cause scission of the PFCB that could be mended thermally by heating. The threshold force for mechanochemical cycloreversion of cyclobutane was studied in single molecule force spectroscopy (SMFS) experiments which showed that the mechanical stress required to activate the cyclobutane mechanophores was tensile.[18] The force-coupled reactivity of multimechanophore polymers bearing cyclobutene was investigated using SMFS to identify force-modified pathways for electrocyclic ring-opening reactions.[19] In another AFM sliding experiment, the decomposition rates of alkyl, vinyl, and acetylide terminated carboxylate species adsorbed on copper were studied and the carbon removal rate was found to depend on the nature of the hydrocarbon terminal group.[20] Studies of shear driven polymerization reactions with simple organic molecules including allyl alcohol, α-pinene, pinane, and n-decane demonstrated the role of surface oxygen, ring strain, and C=C double bond in mechanochemical activation.[21–24]

Although experiments at different length scales have contributed to the understanding of mechanochemical processes, these techniques cannot directly provide the in-situ stress state of the reactant species nor the reaction pathways with atomic resolution. Thus, computational techniques, such as first principles calculations and molecular dynamics (MD) simulations, have been used to complement experiments. First principles calculations can accurately capture the atomic behavior of a system and, thus, quantum mechanics/molecular mechanics (QM/MM) simulations, ab initio calculations, and density functional theory (DFT) calculations have been widely used to study mechanochemical reactions. However, first principles-based studies are computationally expensive, which limits their scope to only a small number of molecules with restricted dynamics. DFT calculations involve no dynamics at all, and thus, cannot be used to study the dynamic evolution of a system. On the other hand, reactive MD simulations with bond order-based potentials are several orders of magnitude faster than first principles approaches, albeit at the expense of some accuracy, allowing much larger systems to be simulated under experimentally relevant conditions. In particular, the ReaxFF force field, which was initially developed to study hydrocarbon reactivity, has been parameterized to model a wide range of chemical systems and processes,[25–27] including mechanochemical reactions.

ReaxFF-MD simulations have been used to study mechanochemical reactions of different organic molecules and substituents. The effect of alkyl substituents on mechanochemical reactions of phosphate esters under shear was studied and it was found that esters with secondary alkyl substituents had much higher dissociation rates than primary substituents.[28] A study of di-tert-butyl disulfide on Fe(100) captured decomposition pathways and showed that the reaction yield at different temperature and pressure conditions could be described by a shear-assisted thermal reaction model.[29,30] ReaxFF-MD simulations of polymerization of allyl alcohol and α-pinene identified shear stress as the key driver of oligomerization reactions and suggested that the mechanochemical activation of the reacting species was caused by shear-induced physical deformation.[21,23,31] A hybrid MD simulation framework integrating a classical force field and ReaxFF captured the physical entanglement between an epoxy network and a cyclobutane-based mechanophore embedded polymer chain, and showed that the intensity of fluorescence was directly proportional to the deformation of the mechanophore.[32] Another study on dimeric anthracene-based mechanophore using the same hybrid MD simulation framework predicted the critical strain for the activation of the mechanophore embedded polymer that was in good agreement with experimental findings.[33] As such, ReaxFF-MD simulations have been shown to be a powerful tool for atomistic investigation of mechanochemical reactions and to provide valuable insights into the molecular mechanisms of mechanical activation.

Here, mechanochemical reactions of a homologous series of simple cyclic organic compounds were studied using ReaxFF-MD to explore the effect of molecular structure on susceptibility to mechanical activation. Previous studies of α-pinene, pinane, and n-decane highlighted the role of ring strain and C=C double bond in shear-driven reactions.[23,24,31] Based on this, we modeled methylcyclopentane, cyclohexane, and cyclohexene to investigate the mechanochemical response of a ring structure, double bond, and methyl side group in cyclic compounds. In the simulations, these precursors were subject to normal and shear stress, and the resulting oxidative chemisorption and oligomerization reactions were tracked. Trends were compared to polymerization yield from ball-on-flat sliding experiments. Finally, the simulations were used to identify and compare oligomerization reaction pathways for the three molecules.

Methods

Computational methods

MD simulations of cyclohexane, cyclohexene, and methylcyclopentane precursors sheared between two silica

surfaces were performed to study the molecular mechanisms of shear-induced reactions (Fig. 1). QuantumATK[34] was used to create three model systems, each containing 50 molecules of one of the three precursors confined between two silica slabs. The number of precursor molecules was chosen to form at least a monolayer on each surface. The amorphous silica slabs were created using a heat and quench method that involved heating a cristobalite slab to 4000 K and then cooling it back to room temperature, with a heating and cooling rate of 0.02 K/fs[23,31]. The cristobalite was placed next to a vacuum region during the amorphization process to form a silica surface with 2 Å average roughness. The surfaces were then passivated by reacting them with water molecules until the number of reactions between the water and the surface reached steady state.

The two silica slabs initially were placed 22 Å apart to minimize interactions between the slabs, provide enough space for the precursor molecules to equilibrate without mechanical stress, and minimize the computational time required to bring the slabs together. Any silica atoms 13.5 Å or farther from the two surfaces were treated as rigid bodies and all other atoms were treated as non-rigid, movable atoms. The initial simulation box dimensions were 33 x 32 x 71 $Å^3$ with periodic boundary conditions in the x- and y-directions and fixed boundaries in the z-direction.

Each MD simulation started with energy minimization and dynamic equilibration at 300 K. The upper slab was then moved towards the bottom slab in the z-direction until the average distance between the two slabs was approximately 10 Å. Then the system was compressed at 1, 3, or 4 GPa pressure for 250 ps by applying load on top of the upper slab. To increase the reactivity of the precursor molecules, the temperature of the system at 4 GPa pressure was increased to 450 K at 1 K/ps rate after the compression stage. Finally, sliding simulations were carried out by moving the upper slab at 10 ms^{-1} speed in the x-direction for 2 ns. The canonical ensemble (NVT) was applied to all non-rigid atoms and charge equilibration was performed throughout the simulation.

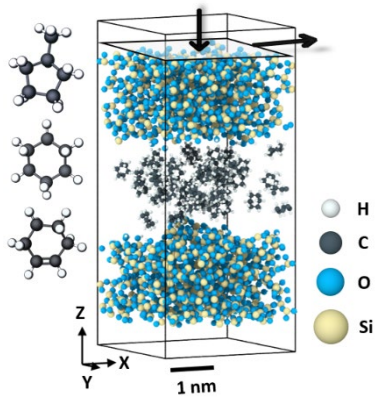

Fig. 1 The model system consisting of methylcyclopentane, cyclohexane, or cyclohexene (shown individually on the left) confined and sheared between amorphous silica slabs. The white, black, blue, and yellow spheres represent H, C, O, and Si atoms, respectively.

The interactions between atoms were modeled using the ReaxFF force field[35,36] with a set of parameters previously developed from a combination of parameters for C/H/O,[37,38] and Si/C interactions.[39] This force field was used for a similar system previously to study thermal and shear-driven oligomerization of α-pinene.[23,31] The time step for dynamics was 0.25 fs. All simulations were performed using the Large Atomic/Molecular Massively Parallel Simulation (LAMMPS) software.[40] Postprocessing was carried out using in-house python scripts and OVITO software.[41]

Experimental details

Shear-induced mechanochemical polymerization reactions of methylcyclopentane, cyclohexane, and cyclohexene were studied with a custom-built environment-controlled ball-on-flat tribometer. The precursor molecules were carried into the tribometer by dry N_2 gas (moisture volume concentration ~ 18 ppm). Adjusting the ratio of the dry N_2 gas stream with the vapor-saturated stream gave a target partial pressure of methylcyclopentane, cyclohexane, or cyclohexene relative to its saturated vapor pressure (P/P_{sat}) at room temperature.[42] The relative partial pressure of all three chemicals was kept at 35% in this experiment. The sliding speed was kept at 3 mm/s. The substrate was prepared by heating a silicon (100) wafer (Wafer World, Inc.) at 450°C for 12 hours. This process grew a thermal oxide layer on a silicon wafer with a low degree of hydroxylation, which is reasonably reactive for mechanochemical oligomerization of adsorbed molecular species.[23] The counter surface was a borosilicate ball (Pyrex; Fisher Scientific) with a diameter of 3 mm. After the tribo-test, polymerization products left on the sliding track were imaged with atomic force microscopy (AFM; Digital instrument, MultiMode). The total volume of reaction products was estimated by calculating the volume of material above the silica surface.[43] To check the reproducibility of the data, the test was repeated three times for each precursor.

Results and discussion

The initial reaction for all precursor molecules was oxidative chemisorption, resulting in a reduction in the number of intact precursor molecules in the system. Fig. 2 shows this reduction in precursor molecules and corresponding increase in the oxidized chemical species. Without sliding (before 0.75 ns), only a few molecules reacted with surface oxygen at any temperature or pressure (Fig. 2 and Fig. S1). The increase in oxidative chemisorption coincided with the onset of sliding, demonstrating that shear stress accelerated oxidative chemisorption of all three precursors. Similar observations have been made for other simple organic molecules, including α-pinene and allyl alcohol, in both experiments and simulations.[21,23,31,43] Here, interesting observations can be made from the relative reactivity of the three precursors.

For methylcyclopentane and cyclohexane at 300 K, very little oxidative chemisorption was observed at any pressure condition tested (Fig. S1). At 4 GPa and 450 K, the reactivity of cyclohexane increased slightly relative to the 300 K cases, but

there was no change in the reactivity of methylcyclopentane. At any temperature and pressure condition, cyclohexene produced the most oxidized species. For cyclohexene, the activation volume was calculated from the reaction rate constant at different shear stresses (see supplementary information) and found to be 5.6 ± 1.5 Å^3, which is comparable to the values reported for polymerization of similar chemical species in previous studies.[21,23,31] Activation volume could not be calculated for cyclohexane or methylcyclopentane due to their low reactivity.

The difference in the reactivity of the three compounds was further investigated by characterizing the oxidative chemisorption at each carbon. Methylcyclopentane, cyclohexane, and cyclohexene molecules have six potential carbon sites (C1-C6) at which oxidative chemisorption reactions can occur. The most reactive site for oxidative chemisorption was identified by calculating the percentage of oxidation reactions that occurred at each carbon site with respect to the total number of oxidation reactions for a given precursor. An oxidation reaction was defined as formation of a covalent bond between a carbon atom and a surface oxygen atom. Data from simulations at all temperature and pressure conditions for each precursor was used for this analysis and the results are shown in Fig. 3.

Especially, the methyl side group (C6) was found to be the most reactive. Cyclohexane is a symmetrical molecule, so all six carbon atoms of the molecule should have relatively equal probability of participating in an oxidation reaction. However, the distribution in Fig. 3 is not symmetric, likely due to the small number of total oxidation reactions observed in the cyclohexane simulations (Fig. 2 and Fig. S1). Finally, for cyclohexene, about 80% of all oxidation reactions happened at the double bond sites (C1 and C2), indicating that the C=C double bond is very susceptible to mechanochemical activation. The probabilities calculated for cyclohexene are statistically more significant than the other two precursors due to the much higher number of observed cases of cyclohexene oxidation reactions (Fig. 2, Fig. S1).

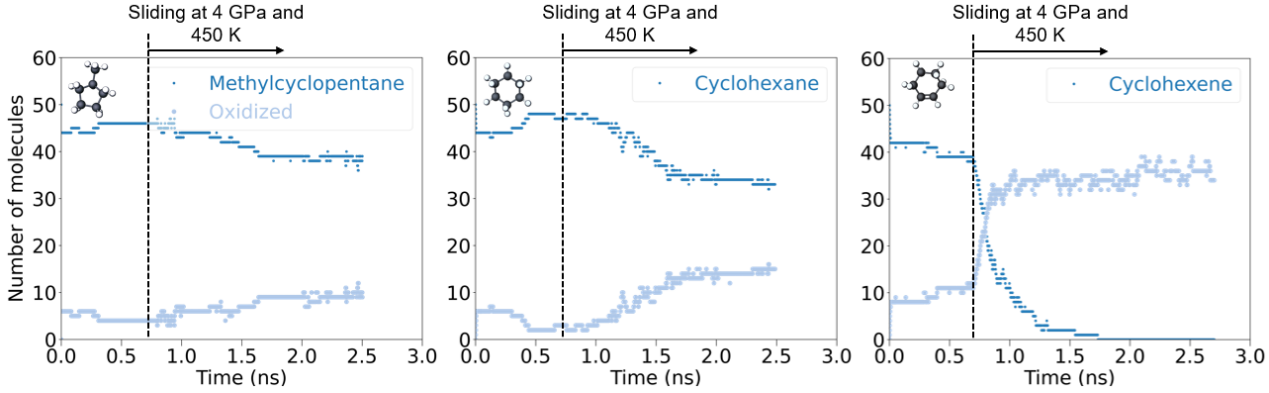

Fig. 2 Evolution of the number of intact methylcyclopentane, cyclohexane, and cyclohexene molecules and corresponding change in the number of oxidized species in simulations at 4 GPa and 450 K. Sliding started from 0.75 ns, after the system was equilibrated, compressed to 4 GPa, and heated from 300 K to 450 K.

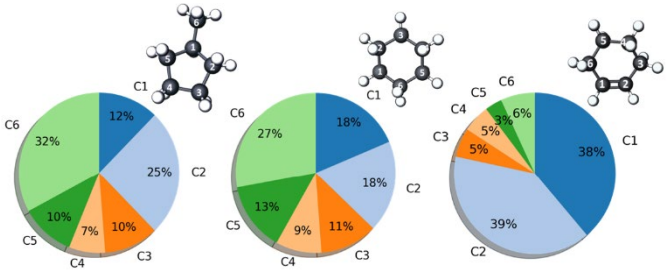

Fig. 3 Probability of each carbon site on the three precursors participating in an oxidative chemisorption reaction. Data from all four pressure and temperature condition simulations was used in the analysis for each precursor.

For methylcyclopentane, the C2, C5, and C6 carbon sites neighboring the tertiary C1 site accounted for 67% of all methylcyclopentane oxidation reactions, which suggests that these sites are more responsive to mechanochemical activation.

Oxidative chemisorption has been shown previously to precede polymerization or oligomerization in both tribometer experiments and simulations.[21,23,24,31,43] Fig. 4 shows the evolution of oligomers in the simulations for the three precursors at 4 GPa pressure and 450 K. For all three precursors, no oligomers formed before sliding started, which indicated that oligomerization of the molecules was mainly driven by shear stress. Fewer than three oligomers were detected for either methylcyclopentane or cyclohexane after sliding for 2 ns. In contrast, about eight oligomers formed during the same time

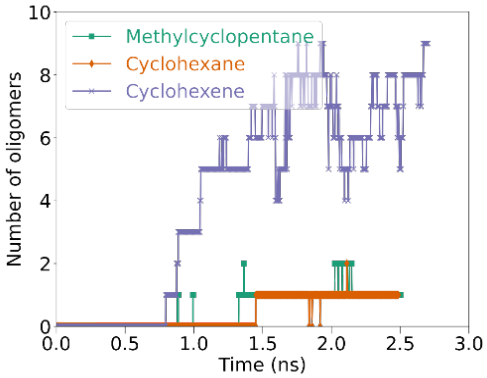

Fig. 4 Number of oligomers in simulations of methylcyclopentane, cyclohexane, and cyclohexene at 4 GPa and 450 K. Sliding started at 0.75 ns.

for cyclohexene (Fig. 4). The oligomerization trends are consistent with those observed for oxidation. This suggests that oxidation is the first step in the oligomerization reaction pathway, as observed previously for shear-driven association reactions of α-pinene.[31]

To confirm the trends observed in the simulations, experiments with the similar conditions were carried out. Fig. 5 shows AFM images of one end and the middle of the sliding tracks after 600 reciprocating sliding cycles. The line profiles of the middle of sliding track show more accumulation of reaction products for cyclohexene than the other two precursors. We estimated the amount of reaction product from the volume of material above the silica reference plane to be (16.1±6.6)×10^3, (8.7±2.9)×10^3, and (45.9±5.8)×10^3 μm^3 in methylcyclopentane, cyclohexane, and cyclohexene, respectively. The experimental reaction products were polymeric species, and so not directly comparable to the results for dimers in the simulations. However, the much larger reaction product yield for cyclohexene in the experiments is qualitatively consistent with trends in the simulations (Fig. 4). This indicates that the simulations reproduced the comparative reactivity of the three precursors during mechanochemical excitation.

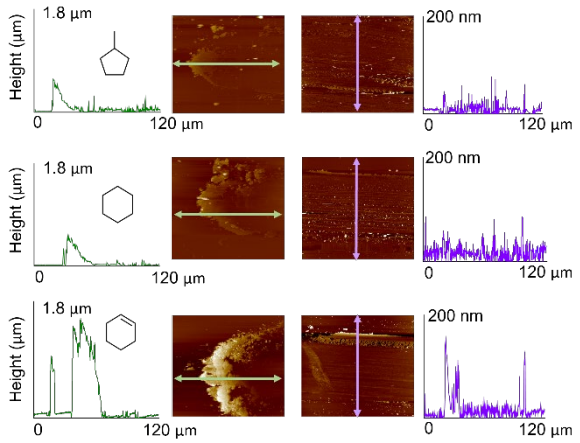

Fig 5 AFM images and the height profiles of the reaction products accumulated at the ends (left) and the middle (right) of the sliding track after the shear-induced mechanochemical reactions of methylcyclopentane, cyclohexane, and cyclohexene. The size of the images is 120 × 120 μm^2.

Next, the simulated oligomerization reaction pathways of all three precursors were investigated to identify the molecular mechanisms of mechanochemical activation. Fig. 6 shows snapshots of the key steps of the oligomerization reaction pathways for methylcyclopentane, cyclohexane, and cyclohexene. Both methylcyclopentane and cyclohexane followed a similar pathway, which began through hydrogen elimination of an intact precursor molecule. The hydrogen elimination reaction happened between a surface siloxane and a precursor molecule, eventually forming silanol and an undercoordinated carbon atom. These undercoordinated atoms are identified by red asterisks in Fig. 6. In the case of methylcyclopentane, the carbon at the methyl group (C6) was the most reactive site for the hydrogen elimination, whereas all six carbon atoms of cyclohexane were equally likely to undergo hydrogen elimination. Next, the undercoordinated carbon atom reacted with another surface oxygen, identified by a small black circle in Fig. 6, resulting oxidative chemisorption of the radical. This second step could happen through reaction with either a surface silanol or a siloxane group. Finally, a second hydrogen-deficient or oxidized precursor reacted with the first oxidized species to form an oligomer through an ether linkage.

In contrast, cyclohexene followed a reaction pathway that involved direct activation of the double bond site to form oligomers. Cyclohexene oligomerization reactions started with

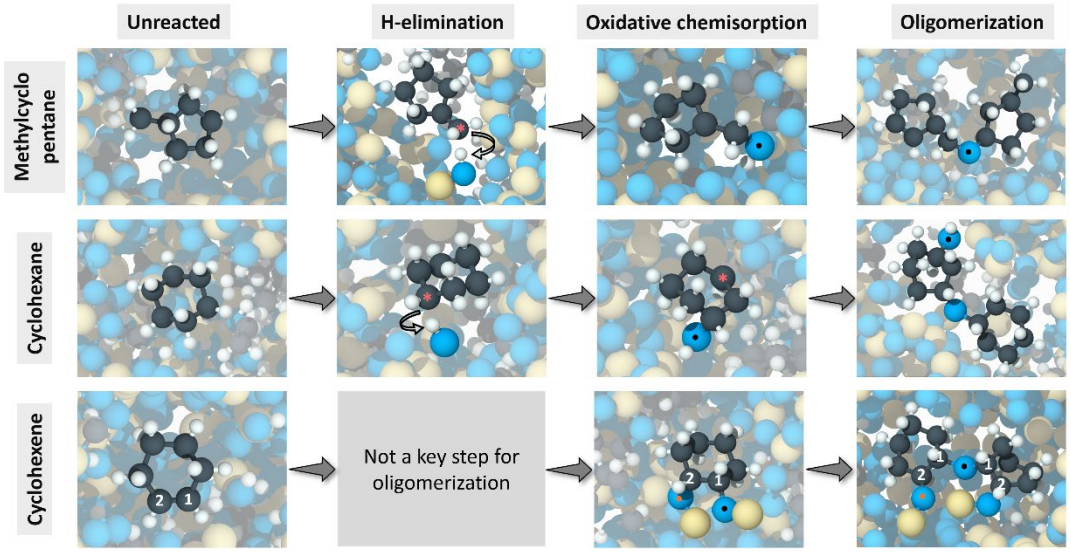

Fig. 6: Simulation snapshots showing the key steps of the oligomerization reaction pathways for the three precursors. Although hydrogen elimination was a key step for oligomerization of methylcyclopentane and cyclohexane, all observed oligomerization reactions of cyclohexene involved direct oxidation at the double bond site (C1=C2). Undercoordinated C atoms are identified with red asterisks in the snapshots. Oxygen atoms shown in consecutive snapshots of a pathway are identified with black or orange dots. From left to right, the snapshots were taken approximately at simulation times of 0, 1.0, 1.3, and 1.6 ns for methylcyclopentane; 0, 1.1, 1.3, and 1.5 ns for cyclohexane; and 0, 0.7, and 0.9 ns for cyclohexene.

oxidative chemisorption of an intact molecule at one or both double bond sites. This is shown in Fig. 6 as carbon atoms labeled 1 and 2 bonding with oxygen atoms identified with small orange or black circles. Then, another intact or oxidized cyclohexene molecule reacted with the first reactant to form an ether linkage. This, in turn, resulted in the formation of an oligomer. Although cyclohexene could undergo hydrogen elimination followed by oxidation like the two other precursors, no oligomer was observed to form through this pathway. Note that, since surface oxygen atoms played a crucial role in all oligomerization reactions, the presence of chemical species such as water or oxygen at the interface may affect the oligomerization reaction pathways,[43] although this could not be studied using the present model systems.

To investigate if the shear-driven reactions or reaction mechanisms described above could be driven thermally, simulations without applied normal or shear stress were run at 900 K for all three precursors. Methylcylopentane and cyclohexane remained unreactive with no oxidative chemisorption observed (Fig. S4). Cyclohexene exhibited some oxidation at 900 K, but the reaction rate was much lower than observed in the sliding simulations at room temperature at any normal stress. No oligomers were observed in any of the heating simulations, suggesting that the thermal energy needed for oligomerization was higher than the energy available at 900 K. Since no oligomers formed thermally, direct comparison between thermal and shear-driven reaction pathways could not be made. However, in previous study of α-pinene using a similar model system, oligomerization reaction pathways and reaction intermediates at temperatures above 900 K were found to differ from shear-activated pathways.[31]

Conclusions

In this work, mechanochemical activation of methylcyclopentane, cyclohexane, and cyclohexene molecules subject to compression and shear at a silica interface was studied using reactive MD simulations. The precursor molecules reacted with surface oxygen atoms to undergo oxidative chemisorption reactions that were mainly driven by shear stress. Methylcyclopentane and cyclohexane exhibited low responsiveness to mechanical activation since the yield of oxidative chemisorption for these precursors was quite low even at high pressure and elevated temperature. In contrast, cyclohexene was found to be very sensitive to mechanical activation, participating in many oxidative chemisorption reactions at all simulated pressure and temperature conditions. Analyzing the chemisorbed molecules revealed that the difference in the reactivity of the precursor molecules stemmed from the difference in their chemical features. In the case of methylcyclopentane, most of the oxidation reactions happened at the methyl group side of the molecule, whereas, for cyclohexene, about 80% of all oxidation reactions happened at the double bond sites. Oxidative chemisorption of the precursor molecules eventually led to oligomer formation and cyclohexene was observed to form the most oligomers at all pressure and temperature conditions. This trend was in qualitative agreement with the tribopolymer yield observed in ball-on-flat tribometer experiments. Analyzing the oligomerization reaction pathways showed that both methylcyclopentane and cyclohexane followed a similar mechanism of hydrogen elimination followed by oxidation and, finally, oligomerization. Cyclohexene, however, did not require hydrogen elimination to form oligomers since direct oxidation at the double bond sites facilitated oligomerization. The results of this study show how chemical structure can change the mechanical activation mode and may also suggest ways to introduce chemical species as mechanophores in polymers or substituents in stress-activated reactants to tune reactivity.

Author Contributions

F. H. Bhuiyan: Simulations, analysis, and writing; Y.-S. Li: AFM experiments; S. H. Kim: Conceptualization, review, editing; A. Martini: Supervision, writing, review, editing.

Conflicts of interest

There are no conflicts of interest to declare.

Acknowledgements

This work was supported by the National Science Foundation (Grant No. CMMI-2038494 and 2038499). The authors thank Arash Khajeh for providing the amorphous silica surfaces used in the simulations.

References

1 J.-L. Do and T. Friščić, *ACS Cent Sci*, 2017, **3**, 13–19.
2 S. Mateti, M. Mathesh, Z. Liu, T. Tao, T. Ramireddy, A. M. Glushenkov, W. Yang and Y. I. Chen, *Chem. Commun.* , 2021, **57**, 1080–1092.
3 J. Andersen and J. Mack, *Green Chem.*, 2018, **20**, 1435–1443.
4 H. Lee, D. Lee and H. Jeong, *International Journal of Precision Engineering and Manufacturing*, 2016, **17**, 525–536.
5 Y. Chen, G. Mellot, D. van Luijk, C. Creton and R. P. Sijbesma, *Chem. Soc. Rev.*, 2021, **50**, 4100–4140.
6 M. A. Ghanem, A. Basu, R. Behrou, N. Boechler, A. J. Boydston, S. L. Craig, Y. Lin, B. E. Lynde, A. Nelson, H. Shen and D. W. Storti, *Nature Reviews Materials*, 2020, **6**, 84–98.
7 X. Chen, K. Kawai, H. Zhang, K. Fukuzawa, N. Koga, S. Itoh and N. Azuma, *J. Phys. Chem. C*, 2020, **124**, 22496–22505.
8 H. Spikes, *Friction*, 2018, **6**, 1–31.
9 W. Tysoe, *Tribol. Lett.*, 2017, **65**, 48.
10 N. N. Gosvami, J. A. Bares, F. Mangolini, A. R. Konicek, D. G. Yablon and R. W. Carpick, *Science*, 2015, **348**, 102–106.
11 J. Zhang and H. Spikes, *Tribol. Lett.*, 2016, **63**, 24.
12 J. Zhang, J. P. Ewen, M. Ueda, J. S. S. Wong and H. A. Spikes, *ACS Appl. Mater. Interfaces*, 2020, **12**, 6662–6676.
13 D. A. Davis, A. Hamilton, J. Yang, L. D. Cremar, D. Van Gough, S. L. Potisek, M. T. Ong, P. V. Braun, T. J. Martínez, S. R. White, J. S. Moore and N. R. Sottos, *Nature*, 2009, **459**, 68–72.

14 K. Hoshino, K. Yagishita, K. Tagawa and H. Spikes, *SAE International Journal of Fuels and Lubricants; Warrendale*, 2012, **5**, 504–510.
15 S. Wang, H. K. Beech, B. H. Bowser, T. B. Kouznetsova, B. D. Olsen, M. Rubinstein and S. L. Craig, *J. Am. Chem. Soc.*, 2021, **143**, 3714–3718.
16 M. Sommer, *Macromol. Rapid Commun.*, 2021, **42**, 2000597.
17 H. M. Klukovich, Z. S. Kean, S. T. Iacono and S. L. Craig, *J. Am. Chem. Soc.*, 2011, **133**, 17882–17888.
18 M. F. Pill, K. Holz, N. Preußke, F. Berger, H. Clausen-Schaumann, U. Lüning and M. K. Beyer, *Chemistry*, 2016, **22**, 12034–12039.
19 C. L. Brown, B. H. Bowser, J. Meisner, T. B. Kouznetsova, S. Seritan, T. J. Martinez and S. L. Craig, *J. Am. Chem. Soc.*, 2021, **143**, 3846–3855.
20 R. Rana, R. Bavisotto, K. Hou, N. Hopper and W. T. Tysoe, *Tribol. Lett.*, 2021, **70**, 5.
21 J. Yeon, X. He, A. Martini and S. H. Kim, *ACS Appl. Mater. Interfaces*, 2017, **9**, 3142–3148.
22 X. He and S. H. Kim, *Langmuir*, 2017, **33**, 2717–2724.
23 A. Khajeh, X. He, J. Yeon, S. H. Kim and A. Martini, *Langmuir*, 2018, **34**, 5971–5977.
24 X. He, A. J. Barthel and S. H. Kim, *Surf. Sci.*, 2016, **648**, 352–359.
25 A. Martini and S. H. Kim, *Tribol. Lett.*, 2021, **69**, 150.
26 H. Carlton, D. Huitink and H. Liang, *Lubricants*, 2020, **8**, 87.
27 A. Martini, S. J. Eder and N. Dörr, *Lubricants*, 2020, **8**, 44.
28 C. Ayestarán Latorre, J. E. Remias, J. D. Moore, H. A. Spikes, D. Dini and J. P. Ewen, *Communications Chemistry*, 2021, **4**, 1–11.
29 K. Mohammadtabar, S. J. Eder, P. O. Bedolla, N. Dörr and A. Martini, *Langmuir*, 2018, **34**, 15681–15688.
30 K. Mohammadtabar, S. J. Eder, N. Dörr and A. Martini, *J. Phys. Chem. C Nanomater. Interfaces*, 2019, **123**, 19688–19692.
31 F. H. Bhuiyan, S. H. Kim and A. Martini, *Appl. Surf. Sci.*, 2022, **591**, 153209.
32 B. Koo, A. Chattopadhyay and L. Dai, *Comput. Mater. Sci.*, 2016, **120**, 135–141.
33 B. Koo, E. Nofen, A. Chattopadhyay and L. Dai, *Comput. Mater. Sci.*, 2017, **133**, 167–174.
34 S. Smidstrup, T. Markussen, P. Vancraeyveld, J. Wellendorff, J. Schneider, T. Gunst, B. Verstichel, D. Stradi, P. A. Khomyakov, U. G. Vej-Hansen, M.-E. Lee, S. T. Chill, F. Rasmussen, G. Penazzi, F. Corsetti, A. Ojanperä, K. Jensen, M. L. N. Palsgaard, U. Martinez, A. Blom, M. Brandbyge and K. Stokbro, *J. Phys. Condens. Matter*, 2020, **32**, 015901.
35 T. P. Senftle, S. Hong, M. M. Islam, S. B. Kylasa, Y. Zheng, Y. K. Shin, C. Junkermeier, R. Engel-Herbert, M. J. Janik, H. M. Aktulga, T. Verstraelen, A. Grama and A. C. T. van Duin, *npj Computational Materials*, 2016, **2**, 1–14.
36 A. C. Chipara, T. Tsafack, P. S. Owuor, J. Yeon, C. E. Junkermeier, A. C. T. van Duin, S. Bhowmick, S. A. S. Asif, S. Radhakrishnan, J. H. Park, G. Brunetto, B. A. Kaipparettu, D. S. Galvão, M. Chipara, J. Lou, H. H. Tsang, M. Dubey, R. Vajtai, C. S. Tiwary and P. M. Ajayan, *Materials Today Chemistry*, 2018, **9**, 149–157.
37 S. G. Srinivasan and A. C. T. van Duin, *J. Phys. Chem. A*, 2011, **115**, 13269–13280.
38 K. Chenoweth, A. C. T. van Duin and W. A. Goddard 3rd, *J. Phys. Chem. A*, 2008, **112**, 1040–1053.
39 K. Chenoweth, S. Cheung, A. C. T. van Duin, W. A. Goddard 3rd and E. M. Kober, *J. Am. Chem. Soc.*, 2005, **127**, 7192–7202.
40 S. Plimpton, *J. Comput. Phys.*, 1995, **117**, 1–19.
41 A. Stukowski, *Modell. Simul. Mater. Sci. Eng.*, 2009, **18**, 015012.
42 D. B. Asay and S. H. Kim, *J. Phys. Chem. B*, 2005, **109**, 16760–16763.
43 X. He, A. Pollock and S. H. Kim, *Tribol. Lett.*, 2019, **67**, 25.